

Short communication

Nanostructured Pt/C and Pd/C catalysts for direct formic acid fuel cells

Zhaolin Liu^{a,*}, Liang Hong^{a,b}, Mun Pun Tham^a, Tze Han Lim^a, Huixin Jiang^a

^a Institute of Materials Research & Engineering, 3 Research Link, Singapore 117602, Singapore

^b Department of Chemical and Biomolecular Engineering, National University of Singapore, 10 Kent Ridge Crescent, Singapore 119260, Singapore

Received 7 March 2006; accepted 29 May 2006

Available online 27 July 2006

Abstract

Platinum (Pt) and palladium (Pd) nanoparticles supported on Vulcan XC-72 carbon are prepared by a microwave-assisted polyol process. The catalysts are characterized by transmission electron microscopy and X-ray diffraction analysis. The average particle size of Pt and Pd nanoparticles, which are uniformly dispersed on carbon, is 4 and 5 nm, respectively. The Pt/C and Pd/C catalysts exhibit four diffraction peaks that are indexed to the {111}, {200}, {220}, and {311} planes of Pt and Pd, respectively. The electrooxidation of formic acid is examined by cyclic voltammetry and chronoamperometry. The Pd/C catalyst is found to have a higher electrocatalytic activity for formic acid oxidation than a comparative Pt/C catalyst. Preliminary data from a single-stack test cell of a direct formic acid fuel cell (DFAFC) using Pd/C as the anode catalyst yield high power density.

© 2006 Elsevier B.V. All rights reserved.

Keywords: Platinum nanoparticles; Palladium nanoparticles; Formic acid; Catalytic activity; Fuel cell; Power density

1. Introduction

During the past 20 years, direct methanol fuel cells (DMFCs) have been widely studied and considered as possible power sources for the portable electronic devices and electric vehicles. These fuel cells offer a variety of benefits such as high specific energy and the ready availability and portability of methanol. On the other hand, the problem of methanol ‘crossover’ from the anode to the cathode through the membrane leads to low system efficiency. Methanol crossover prevents utilization of high concentration of methanol; the limits generally less than 2 M. The feasibility of direct formic acid fuel cells (DFAFCs) based on proton exchange membranes has been demonstrated by Masel et al. [1–3]. Hsing et al. [4] have also reported that the rate of fuel crossover can be reduced by a factor of 5 and thus a higher performance can be obtained when formic acid is used in place of methanol under the same conditions.

Carbon-supported Pt catalysts for the electro-oxidation of formic acid are poisoned severely by the adsorbed CO intermediate of the reaction [5–7]. It has been demonstrated [8,9] that

PtRu and PtPd alloys can diminish this CO poisoning effect to some extent, but it still limits significantly the catalytic activity for formic acid oxidation. Recently, Masel et al. [10,11] have disclosed that unsupported Pd and Pd/C catalysts can overcome CO poisoning effect and thereby yield high performances in the DFAFCs.

It is well known that catalytic activity is strongly dependent on the shape, size and distribution of the metal particles [12]. Conventional preparation techniques based on wet impregnation and chemical reduction of the metal precursors often do not provide adequate control of particle shape and size [12]. Accordingly, there are continuing efforts to develop alternative synthesis methods based on microemulsions [13], sonochemistry [14,15], or microwave irradiation [16–20]. In principle, all of these methods are more conducive to generating colloids and clusters of particles at the nanoscale, and with greater uniformity. For example, Boennemann et al. [21], prepared organoaluminum-stabilized bimetallic colloids with particle sizes smaller than 2 nm and deposited them on a commercial support at room temperature. The stabilizing surfactant shell on the metal particles had to be removed before the metal particles could be used for electrocatalysis. In another approach, first used by Yu and co-workers [16] and generally known as the polyol process, an ethylene glycol solution of the metal

* Corresponding author. Tel.: +65 68727 532; fax: +65 68720 785.
E-mail address: zl-liu@imre.a-star.edu.sg (Z. Liu).

salt was refluxed at 393–443 K to generate *in situ* reducing species from ethylene glycol for the reduction of the metallic species. Conductive heating is often used but microwave dielectric loss heating may be a better synthesis option in view of its energy efficiency, speed, uniformity, and simplicity in execution [22].

In this work, a simple microwave-assisted polyol procedure is adopted for preparing Pt and Pd nanoparticles supported on activated carbon. The physicochemical properties and electrochemical activities of the nanoparticles for formic acid oxidation are investigated.

2. Experimental

The Pt/C (30 wt.% Pt on Cabot Vulcan XC-72) and Pd/C (30 wt.% Pd on Cabot Vulcan XC-72) catalysts were prepared by microwave heating of ethylene glycol (EG) solutions of the Pt or Pd salt. A typical preparation would consist of the following step. In a 100-ml beaker, 1.0 ml of an aqueous solution of 0.05 M $\text{H}_2\text{PtCl}_6 \cdot 6\text{H}_2\text{O}$ (Aldrich, A.C.S. Reagent) or 0.05 M PdCl_2 was mixed with 25 ml of ethylene glycol (Mallinckrodt, AR). Next, 0.4 M KOH was added drop wise to give a total volume of 0.75 (or 0.25 ml) and then 0.040 g of Vulcan XC-72 carbon with a specific BET surface-area of $250 \text{ m}^2 \text{ g}^{-1}$ and an average particle size of 40 nm was added to the mixture and sonicated. The beaker and its contents were heated in a house-hold microwave oven (National NN-S327WF, 2450 MHz, 700 W) for 50 s. The resulting suspension was filtered and the residue was washed with acetone and dried at 373 K overnight in a vacuum oven.

The catalysts were examined by transmission electron microscopy (TEM) on a JEOL JEM 2010 instrument. For microscopic examinations, the samples were first ultrasonicated in acetone for 1 h and then deposited on 3-mm copper grids that were covered by a continuous carbon film. X-ray diffraction (XRD) patterns were recorded with a Bruker GADDS diffractometer with an area detector that used a $\text{Cu K}\alpha$ source ($\lambda = 1.54056 \text{ \AA}$) operating at 40 kV and 40 mA. The XRD samples were obtained by depositing carbon-supported nanoparticles on a glass slide and then drying overnight under vacuum.

An EG&G Model 263A potentiostat/galvanostat and a conventional three-electrode test cell were used for electrochemical measurements. The working electrode was a thin layer of Nafion-impregnated catalyst cast on a vitreous carbon disc held in a Teflon cylinder. The catalyst layer was obtained in the following way: (i) a slurry was first prepared by sonicating for 1 h a mixture of 0.5 ml of deionized water, 13 mg of Pt/C and Pd/C catalyst, and 0.2 ml of Nafion solution (Aldrich: 5 w/o Nafion); (ii) $2 \mu\text{l}$ of the slurry were pipetted and spread on the carbon disc; (iii) the electrode was dried at 90°C for 1 h and mounted on a stainless-steel support. The surface area of the vitreous carbon disc was 0.25 cm^2 and the catalyst loading was 0.15 mg cm^{-2} based on this geometric area. A Pt gauze and an Ag|AgCl electrode were used as the counter and reference electrodes, respectively. All potentials are quoted against the Ag|AgCl reference. For cyclic voltammetry and chronoamperometry of methanol oxidation, the electrolyte solution was 3 M

HCOOH in 1 M H_2SO_4 , which was prepared from high-purity sulfuric acid, high-purity grade formic acid, and distilled water.

The MEA (membrane electrode assembly) for the DFAFC test cell was made by hot-pressing pretreated Nafion[®]112 together with an anode sheet and a cathode sheet. The anode sheet was a carbon paper (SGL, Germany) with a carbon-supported Pt or Pd catalyst layer. The cathode sheet was a carbon paper with a carbon-supported 40 wt.% Pt catalyst layer supplied by E-TEK. The catalyst loadings at the anode and cathode were 8 and 4 mg cm^{-2} respectively and the effective electrode area was 6 cm^2 . The fuel was 3 M HCOOH delivered at 2 ml min^{-1} by a micropump and the oxygen flow was regulated by a flowmeter at $500 \text{ cm}^3 \text{ min}^{-1}$.

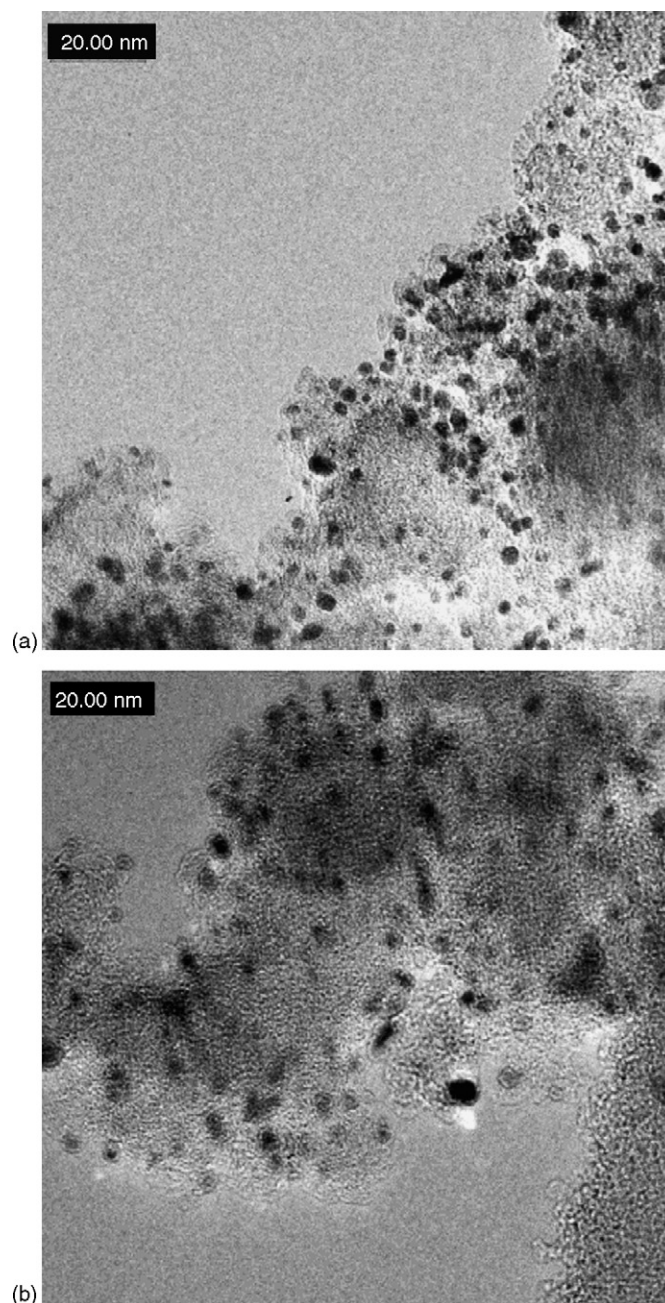


Fig. 1. TEM images of microwave-synthesized Pt/C and Pd/C catalysts: (a) Pt/C; (b) Pd/C.

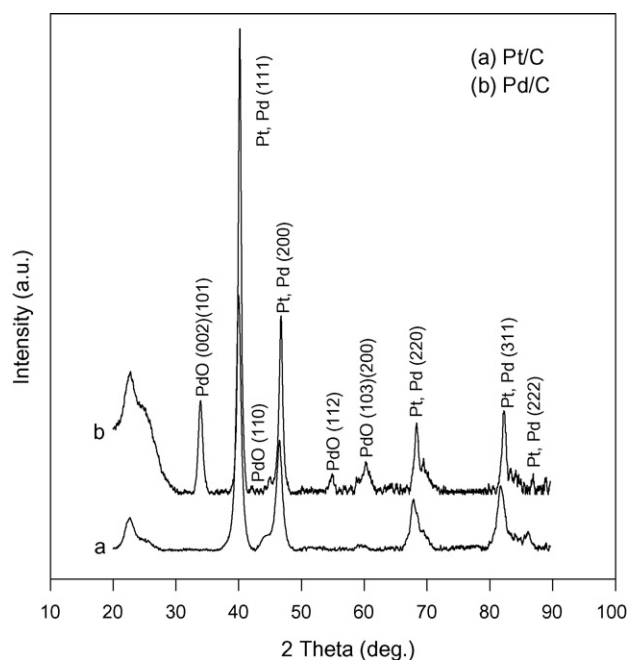


Fig. 2. XRD patterns of microwave-synthesized Pt/C and Pd/C catalysts.

3. Results and discussion

Typical TEM images of the Pt/C and Pd/C catalysts (Fig. 1) show a remarkably uniform and high dispersion of metal particles on the carbon surface with an average particle diameter of 4.0 and 5.0 nm for Pt/C or Pd/C, respectively. Evidently, the microwave-assisted heating of H_2PtCl_6 and PdCl_2 in ethylene glycol has facilitated the formation of smaller and more uniform Pt or Pd particles with good dispersion on the Vulcan carbon support.

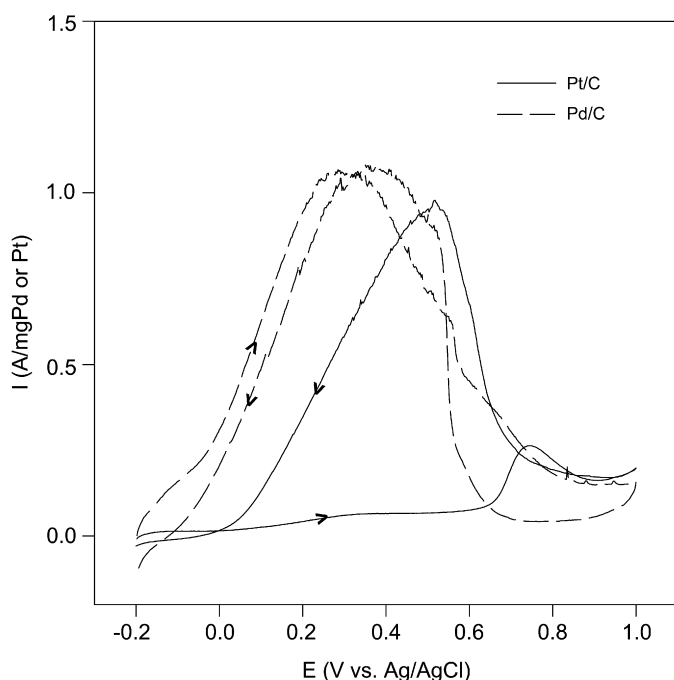


Fig. 3. Cyclic voltammograms of microwave-synthesized Pt/C and Pd/C catalysts in 3 M HCOOH, 1 M H_2SO_4 at a scan rate of 10 mV s^{-1} at 25°C .

It is generally agreed that the size of metal nanoparticles is determined by the rate of reduction of the metal precursor. The dielectric constant (41.4 at 25°C) and the dielectric loss of ethylene glycol are high, and hence rapid heating occurs easily under microwave irradiation [23]. In ethylene glycol mediated reactions (the ‘polyol’ process), ethylene glycol also acts as a reducing agent to reduce the metal ion to metal powder [24]. The fast heating by microwave accelerates the reduction of the metal precursor and the nucleation of the metal clusters. This easing of the nucleation-limited process greatly assists the formation of small particles. Additionally, the homogeneous microwave heating of liquid samples reduces the temperature and concentration gradients in the reaction medium, and thus provides a more uniform environment for the nucleation and growth of metal particles. The carbon surface may contain sites suitable for heterogeneous nucleation and the presence of a carbon surface interrupts particle growth. The smaller and nearly single-dispersed Pt and Pd nanoparticles on carbon XC-72 prepared by microwave irradiation can be rationalized in terms of these general principles.

The XRD patterns (Fig. 2) for Pt/C and Pd/C catalysts show four diffraction peaks that are indexed to the $\{111\}$, $\{200\}$, $\{220\}$, and $\{311\}$ planes of the Pt and the Pd face-centered cubic (fcc) crystal structure, respectively. Except for the reflections of the metallic fcc-phase, the XRD pattern of the Pd/C catalyst displays reflections of the tetragonal PdO-phase. The strong diffraction at $2\theta < 30^\circ$ pertains mostly to the carbon black support. From the XRD patterns, the mean particle sizes were calculated by means of the Scherrer equation [25]:

$$d (\text{\AA}) = \frac{k\lambda}{\beta \cos \theta} \quad (1)$$

where k is a coefficient (0.9), λ the wavelength of X-ray used (1.54056\AA), β the full-width half-maximum of respec-

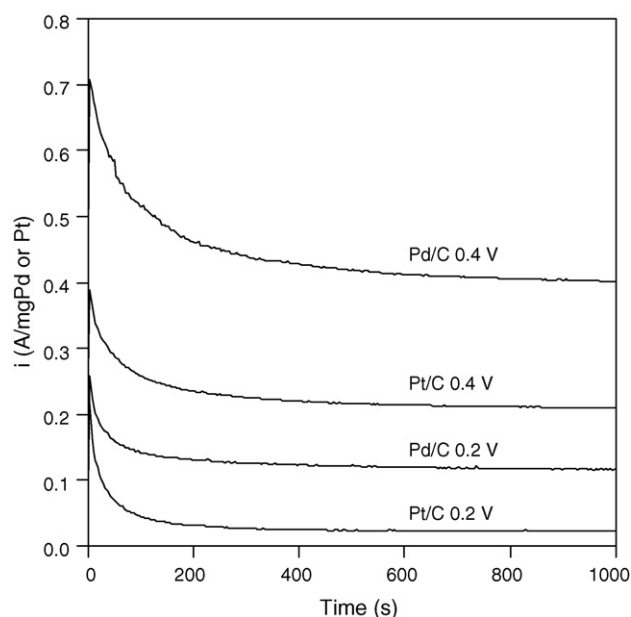


Fig. 4. Polarization current vs. time plots for electrooxidation of formic acid in 3 M HCOOH, 1 M H_2SO_4 electrolyte at 0.4 and 0.2 V at 25°C .

tive diffraction peak and θ is the angle at position of peak maximum.

The mean particle size obtained from the XRD patterns are 3.6 nm for Pt/C and 4.7 nm for Pd/C. Thus, these values of the mean particle size are slightly lower than those obtained above by TEM analysis.

Cyclic voltammograms of formic acid oxidation on Pt/C and Pd/C catalysts are given in Fig. 3. For the Pt/C catalyst, the reaction commences in the hydrogen region and proceeds slowly during the forward scan direction to reach a plateau at 0.3 V. This corresponds to formic acid oxidation through the dehydrogenation path, but the coverage by CO_{ads} simultaneously continues to grow and causes only relatively small

currents [26]. At potentials more positive than 0.65 V, the reaction becomes significantly accelerated and an anodic peak emerges at 0.75 V. The latter can be attributed to the oxidative removal of CO_{ads} together with oxidation of formic acid on sites that were previously blocked by CO_{ads} . At higher potentials, formic acid oxidation is deactivated as result of Pt surface oxidation. On the reversing the potential scan, the surface remains inactive until partial reduction of the irreversibly formed surface oxides. One cathodic peak near 0.5 V is observed, and is due to the oxidation of formic acid after reduction of Pt oxides. For the Pd/C catalyst, the formic acid oxidation shifts to a lower potential and this indicates better electrocatalytic activity.

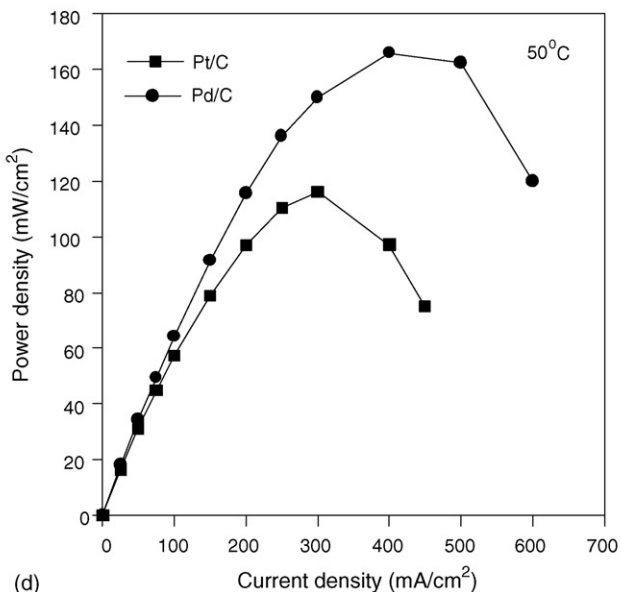
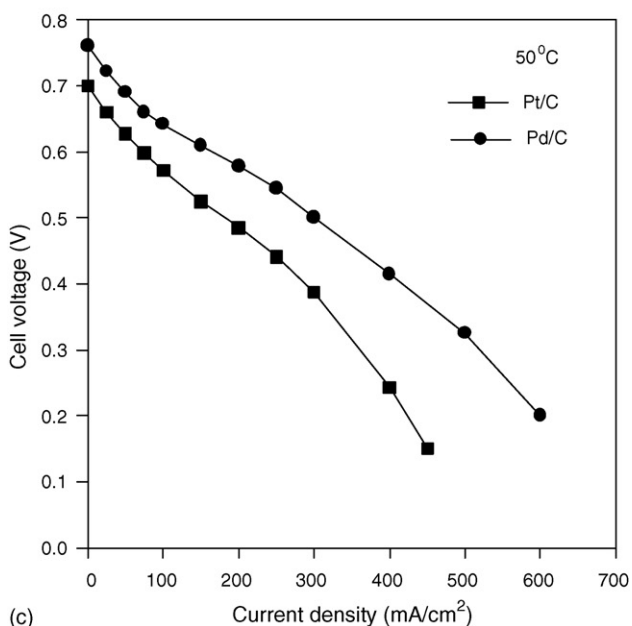
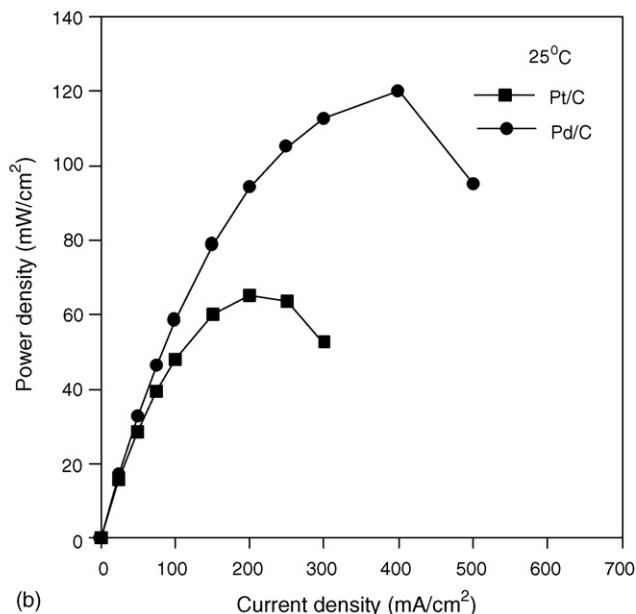
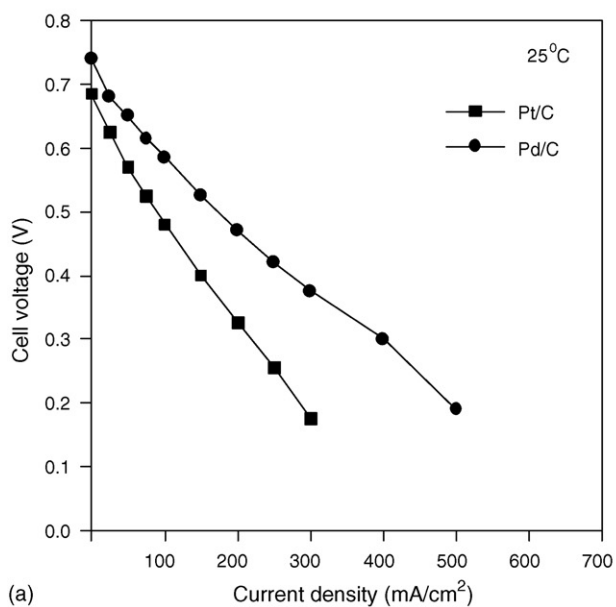


Fig. 5. Polarization curves and output powers of single cell at operating temperature of 25 °C (a and b) and 50 °C (c and d). Anode: Pt/C or Pd/C (8 mg cm⁻²), 3 M HCOOH, 2 ml min⁻¹. Cathode: Pt/C (E-TEK) (4 mg cm⁻²), O₂ 500 cm³ min⁻¹.

The Pd/C and Pt/C catalysts were biased at 0.4 and 0.2 V versus Ag|AgCl and the changes in their polarization currents with time were recorded (Fig. 4). Both catalysts give appreciable current densities at these applied potentials, consistent with the voltammograms in Fig. 3. An initial decrease in the current density with time is found for both catalysts. The current density stabilized within 400 s after application of the set potential. At 0.4 V, the current density for the Pd/C catalyst is about two orders larger than that for the Pt/C catalyst. At 0.2 V, the Pd/C catalyst gives a current density that is about four times higher than that for the Pt/C catalyst. Formic acid oxidation obeys a dual-path mechanism [27–29], namely: (i) dehydrogenation in which formic acid is oxidized directly into CO₂; (ii) dehydration, which involves the CO_{ads} intermediate. The oxidative removal of CO_{ads} occurs at higher potentials. The higher electroactivity of the Pd/C catalyst towards formic acid oxidation suggests that it promotes dehydrogenation without the formation of a surface-poisoning CO_{ads} intermediate.

Polarization and power density curves of single cells with Pt/C and Pd/C catalysts as anode catalysts are shown in Fig. 5. As identified in the cyclic voltammetry and chronoamperometry tests, the Pd/C catalyst is found to exhibit higher activity. At 25 °C, the open-circuit voltages of the cells using Pd/C and Pt/C catalysts are 0.74 and 0.685 V, respectively, while the corresponding peak power densities are 120 and 76.5 mW cm⁻². The power density increases with raising the temperature from 25 to 50 °C, i.e., the peak values for Pd/C and Pt/C catalysts at 50 °C are 166 and 116 mW cm⁻², respectively.

4. Conclusions

A microwave-assisted, rapid heating method is used to prepare carbon-supported Pt and Pd nanoparticles as catalysts for formic acid oxidation in direct formic acid fuel cells (DFAFCs). The preparation is simple, fast and energy efficient, and can be used as a general method for the preparation of other supported metal and alloy systems where the metal precursors are susceptible to the polyol process. The resulting Pt and Pd particles are nanosized (4 nm for Pt/C, 5 nm for Pd/C). The Pt/C and Pd/C catalysts give diffraction patterns for the corresponding Pt and Pd face-centered cubic (fcc) crystal structures. Except for the reflections of the metallic fcc-phase, the XRD pattern for the Pd/C catalyst contains the reflections of tetragonal PdO-phase. Cyclic voltammetry and chronoamperometry tests indicate better electrocatalytic activity for the Pd/C catalyst in formic acid oxidation. From preliminary data collected from

a DFAFC single test cell, which yields high power density, the microwave-prepared Pd/C catalyst is the more promising anode catalyst.

References

- [1] C. Rice, S. Ha, R.I. Masel, P. Waszczuk, A. Wieckowski, T. Barnard, J. Power Sources 111 (2002) 83.
- [2] C. Rice, S. Ha, R.I. Masel, A. Wieckowski, J. Power Sources 115 (2003) 229.
- [3] Y. Zhu, S. Ha, R.I. Masel, J. Power Sources 130 (2004) 8.
- [4] X. Wang, J.M. Hu, I.M. Hsing, J. Electroanal. Chem. 562 (2004) 73.
- [5] J. Jiang, A. Kucernak, J. Electroanal. Chem. 520 (2002) 64.
- [6] S. Park, Y. Xie, M.J. Weaver, Langmuir 18 (2002) 5792.
- [7] J.D. Lovic, A.V. Tripkovic, S.Lj. Gojkovic, K.Dj. Popovic, D.V. Tripkovic, P. Olszewski, A. Kowal, J. Electroanal. Chem. 581 (2005) 294.
- [8] D. Capon, R. Parsons, J. Electroanal. Chem. 65 (1975) 285.
- [9] M. Arenz, V. Stamenkovic, T.J. Schmidt, K. Wandelt, P.N. Ross, N.M. Markovic, Phys. Chem. Chem. Phys. 5 (2003) 4242.
- [10] S. Ha, R. Larsen, Y. Zhu, R.I. Masel, Fuel Cells 4 (2004) 337.
- [11] S. Ha, R. Larsen, R.I. Masel, J. Power Sources 144 (2005) 28.
- [12] I.S. Armadi, Z.L. Wang, T.C. Green, A. Henglein, M.A. El-Sayed, Science 272 (1996) 1924.
- [13] Z.L. Liu, J.Y. Lee, M. Han, W.X. Chen, L.M. Gan, J. Mater. Chem. 12 (2002) 2453.
- [14] K. Okitsu, A. Yue, S. Tanabe, H. Matsumoto, Chem. Mater. 12 (2002) 3006.
- [15] T. Fujimoto, S. Teraushi, H. Umehara, I. Kojima, W. Henderson, Chem. Mater. 13 (2001) 1057.
- [16] W.Y. Yu, W.X. Tu, H.F. Liu, Langmuir 15 (1999) 6.
- [17] D.R. Baghurst, A.M. Chippindale, D.M.P. Mingos, Nature 332 (1988) 311.
- [18] S. Komarneni, D.S. Li, B. Newalkar, H. Katsuki, A.S. Bhalla, Langmuir 18 (2002) 5959.
- [19] W.X. Chen, J.Y. Lee, Z.L. Liu, Chem. Commun. (2002) 2588.
- [20] Z.L. Liu, J.Y. Lee, W.X. Chen, M. Han, L.M. Gan, Langmuir 20 (2004) 181.
- [21] H. Boennemann, R. Binkmann, P. Britz, U. Endruschat, R. Moertel, U.A. Paulus, G.J. Feldmeyer, T.J. Schmidt, H.A. Gasteiger, R.J. Behm, J. New Mater. Electrochem. Syst. 3 (2000) 199.
- [22] X.L. Zhang, D.O. Hayward, D.M.P. Mingos, Ind. Eng. Chem. Res. 40 (2001) 2810.
- [23] R.C. Weast, Handbook of Chemistry and Physics, 47th ed., The Chemical Rubber Co., Cleveland, Ohio, USA, 1966.
- [24] F. Fievet, J.P. Lagier, B. Blin, B. Beaudoin, M. Figlarz, Solid State Ionics 32/33 (1989) 198.
- [25] B.E. Warren, X-ray Diffraction, Addison-Wesley, Reading, MA, USA, 1996.
- [26] V.M. Jovanovic, D. Tripkovic, A. Tripkovic, A. Kowal, J. Stoch, Electrochem. Commun. 7 (2005) 1039.
- [27] A. Capon, R. Parsons, J. Electroanal. Chem. 45 (1973) 205.
- [28] G.Q. Lu, A. Crown, A. Wieckowski, J. Phys. Chem. B 103 (1999) 9700.
- [29] R.S. Jayashree, J.S. Spendelow, J. Yeom, C. Rastogi, M.A. Shannon, P.J.A. Kenis, Electrochim. Acta 50 (2005) 4674.